Int. J. Electrochem. Sci., 17 **(2022)** Article Number: 220945, doi: 10.20964/2022.09.35

International Journal of ELECTROCHEMICAL SCIENCE
www.electrochemsci.org

Energy Efficiency Management of Coupling System for Molten Carbonate Fuel Cells

Jiajun Wu[1], *Liwei Chen*[2,3,*]

[1] School of Management, Xiamen University, Xiamen Fujian 361005, China
[2] School of Mechanical & Electronic Engineering, Sanming University, Sanming 365004, China;
[3] Department of Mechanical Engineering, University of South Carolina, Columbia, 29208, South Carolina, USA.
[*]E-mail: 125601497@qq.com

Received: 1 June 2022 / *Accepted:* 4 July 2022 / *Published:* 7 August 2022

Molten carbonate fuel cell (MCFC) is a typical high-temperature fuel cell, which generates a large amount of waste heat during its operation. Therefore, in order to achieve the best energy efficiency management of MCFC, the secondary utilization of heat is one of the most important means. The performance of molten carbonate fuel cell system is greatly improved by coupling the bipolar energy device. By means of electrochemistry and non-equilibrium thermodynamics, the analytical expressions of the efficiency and power output of the coupled power system of molten carbonate fuel cell are obtained. In addition, the reasonable performance range of the coupling system of molten carbonate fuel cell was analyzed by strict numerical calculation, and the optimal energy efficiency management scheme was given. The results may provide some theoretical basis for the optimal design and practical operation of MCFC coupling system. At the same time, this method can be easily extended to other similar fuel cell coupling system research.

Keywords: Molten carbonate fuel cell; coupling system; energy efficiency management

1. INTRODUCTION

In the 21st century, the most important test facing mankind is the globalization of energy, environment and economic problems, among which the energy problem has been the main contradiction of human society [1-5]. On the issue of electricity, which is closely related to life, there is increasing pressure to make power generation run in a more efficient, cost-effective and environmentally friendly manner due to rising fuel prices, increasingly severe environmental problems, and current and future environmental regulations [6-9]. Fuel cells have the potential to replace conventional power plants because of their high efficiency and zero levels of harmful emissions [10-

12]. Fuel cell can be applied to industrial cogeneration, household cogeneration system, centralized large-scale power supply, decentralized medium and small scale power supply, submarine, automobile, IT equipment, mobile fuel cell generator and so on. Among the existing fuel cell technologies, MCFC, as a typical high-temperature fuel cell, shows excellent prospects due to its fuel flexibility, high efficiency and high waste heat [13-15].

Molten carbonate fuel cell consists of porous ceramic cathode, porous ceramic electrolyte diaphragm, porous metal anode and metal plate, and its electrolyte is molten carbonate. MCFC has the advantages of higher working temperature and faster reaction speed [16]. The purity of the fuel is relatively low, and the fuel can be reformed in the battery. No precious metal catalyst, low cost; Use liquid electrolyte, easy to operate [17]. MCFC has significant advantages in establishing efficient and environmentally friendly decentralized power stations of 50~10,000 kW. Small MCFC power stations with power generation capacity of about 50kW are mainly used for ground communication and weather stations. MCFC medium-sized power stations with power generation capacity of 200-500kW can be used for cogeneration of heat and power for surface ships, locomotives, hospitals, islands and border defense [18]. MCFC large power stations with power generation capacity of more than 1000kW can be combined with thermal cycle power generation, as regional power supply stations, and can also be connected with the municipal power grid. In addition, MCFC can reduce CO_2 emissions by more than 40% by using natural gas, gas and various hydrocarbons as fuel, and can also achieve cogeneration or combined cycle power generation, increasing fuel efficiency to 70% to 80% [19].

There are many studies on improving the energy efficiency of MCFC. For example, some researchers theoretically calculated and simulated the hybrid power system with MCFC as the thermal engine, and evaluated and optimized the hybrid power system [9]. Other scholars established MCFC-based coupling system models in different ways according to different viewpoints and scales, and the obtained results provided a certain theoretical basis for the development of the actual MCFC-based hybrid model [13]. At the same time, a recent study using a hybrid solid-oxide fuel cell and Stirling engine system to replace a single fuel cell found that the power produced by the coupled system increased by about 10 percent compared to the power produced by a single solid-oxide fuel cell [14]. Stirling engine has become the first choice for secondary energy devices because of its incomparable advantages. Stirling engines would gain economies of scale and could establish a cheap source of electricity [16]. Further utilization of the waste heat generated during MCFC operation by Stirling engine will not only reduce the cost of electricity production, but also reduce the complexity of the manufacturing process compared to other engines [20].

In this paper, the performance of molten carbonate fuel cell system is greatly improved by coupling a bipolar energy device. By means of non-equilibrium thermodynamics and electrochemistry, the analytical expressions of the efficiency and power output of the coupled power system of molten carbonate fuel cell are obtained. In addition, the reasonable performance region of the coupling system of molten carbonate fuel cell was analyzed by strict numerical calculation method, so as to obtain the best energy efficiency management scheme.

2. SYSTEM DESCRIPTION

MCFC is a typical high-temperature fuel cell, which generates a large amount of waste heat during its operation. In order to achieve the best energy efficiency management of MCFC, the secondary utilization of the waste heat is one of the most important means. Therefore, a coupling system consisting of MCFC, a Stirling engine and a regenerator is constructed. In this system, MCFC acts as a high temperature heat source for the secondary energy device, and Stirling engine further utilizes the waste heat generated in MCFC and converts it into output work. The regenerator acts as a countercurrent heat exchanger, which reasonably absorbs part of the waste heat to preheat the reactants to achieve improved energy utilization.

2.1 Model of A Molten Carbonate Fuel Cell

The electrolyte of MCFC is molten carbonate, which is generally a carbonate mixture of alkali metals Li, K, Na and Cs. The diaphragm material is $LiAiO_2$, and the positive electrode and negative electrode are nickel oxide and porous nickel with lithium respectively. The MCFC model presented in this study has been previously reported in Ref. [21]. It works as shown in figure 1. Hydrogen and oxygen need to be continuously supplied to the anode and cathode, respectively, to maintain the entire electrochemical reaction. The carbon dioxide produced during the reaction is transported from the anode to the cathode and continues to participate in the reaction, while the carbonate ions flow from the cathode to the anode. The overall electrochemical reaction equation is:

$$H_2 + \frac{1}{2}O_2 + CO_{2,cat} \rightarrow H_2O + CO_{2,an} + electricity + heat \,, \tag{1}$$

The subscripts “an” and “cat” indicate the anode and cathode of the fuel cell respectively. In order to better quantitatively describe the electrochemical reaction process of MCFC, the thermodynamic working process of fuel cell becomes extremely important. Its basic thermodynamic relation can be expressed as follows:

$$-\Delta \dot{H} = -\frac{\Delta h}{n_e F} jA \,, \tag{2}$$

Where Δh is the molar enthalpy change and can be calculated from the data in Table 1 [21, 22], F is the Faraday constant, n_e represents the number of electrons, j refers to the current density and A is the plate area of MCFC. According to the first law of thermodynamics: $-\Delta H = -\Delta G - T\Delta S$, The total enthalpy change $-\Delta H$ can be divided into two parts, the electrical energy and the heat energy released during the reaction, namely, $-\Delta G$ and $-T\Delta S$, which are representative of electrical energy and thermal energy, respectively. As long as the enthalpy change in the reaction is greater than the Gibbs free energy change, the part of the total energy that cannot be converted into electricity will be released as heat energy. After making clear the relationship between energy transfer and conversion, the output power and efficiency of MCFC can be expressed as follows:

Table 1. Parameters used in the modeling [21, 22].

Parameter	Value
Operating pressure, p_0 (atm)	1
Operating temperature, $T(K)$	893.15
Ambient temperature, $T(K)$	293.15
Activation energy of anode, $E_{act,an}$ $(J\ mol^{-1})$	53500
Activation energy of cathode, $E_{act,cat}$ $(J\ mol^{-1})$	77300
Partial pressure of H_2 in the anode, $p_{H_2,an}(atm)$	0.6
Partial pressure of CO_2 in the anode, $p_{CO_2,an}(atm)$	0.15
Partial pressure of H_2O in the anode, $p_{H_2O,an}(atm)$	0.25
Partial pressure of O_2 in the cathode, $p_{O_2,cat}(atm)$	0.08
Partial pressure of N_2 in the cathode, $p_{N_2,cat}(atm)$	0.59
Partial pressure of CO_2 in the cathode, $p_{CO_2,cat}(atm)$	0.08
Partial pressure of H_2O in the cathode, $p_{H_2O,cat}(atm)$	0.25
Faraday constant, $F(C\ mol^{-1})$	96485
Number of electrons, n_e	2
Universal gas constant, $R\ (J\ mol^{-1}\ K^{-1})$	8.314

$$P_{cell} = U_{cell}\, jA = \left\{ \begin{array}{l} E_0 + \dfrac{RT}{n_e F} \ln\left[\dfrac{p_{H_2,an} \left(p_{O_2,cat} \right)^{1/2} p_{CO_2,cat}}{p_{H_2O,an}\, p_{CO_2,an}} \right] - 2.27\times10^{-9}\, j \exp\left(\dfrac{E_{act,an}}{RT} \right) p_{H_2,an}^{-0.42}\, p_{CO_2,an}^{-0.17}\, p_{H_2O,an}^{-1.0} \\ -7.505\times10^{-10}\, j \exp\left(\dfrac{E_{act,cat}}{RT} \right) p_{O_2,cat}^{-0.43}\, p_{CO_2,cat}^{-0.09} - 0.5\times10^{-4}\, j \exp\left[3016\left(\dfrac{1}{T} - \dfrac{1}{923} \right) \right] \end{array} \right\} jA \quad (3)$$

and

$$\eta_{cell} = \frac{P_{cell}}{-\Delta H}$$

$$= -\frac{n_e F}{\Delta h}\left\{ \begin{array}{l} E_0 + \frac{RT}{n_e F}\ln\left[\frac{p_{H_2,an}\left(p_{O_2,cat}\right)^{1/2} p_{CO_2,cat}}{p_{H_2O,an}\,p_{CO_2,an}}\right] - 2.27\times10^{-9}\, j\exp\left(\frac{E_{act,an}}{RT}\right) p_{H_2,an}^{-0.42}\, p_{CO_2,an}^{-0.17}\, p_{H_2O,an}^{-1.0} \\ -7.505\times10^{-10}\, j\exp\left(\frac{E_{act,cat}}{RT}\right) p_{O_2,cat}^{-0.43}\, p_{CO_2,cat}^{-0.09} - 0.5\times10^{-4}\, j\exp\left[3016\left(\frac{1}{T}-\frac{1}{923}\right)\right] \end{array} \right\} \quad (4)$$

Where is the operating temperature of MCFC, $E_0 = -\Delta G/n_e F$ is the ideal standard potential; R is the universal gas constant; E_{act} is activation energy, p_k is the partial pressure of k gases at anode and cathode.

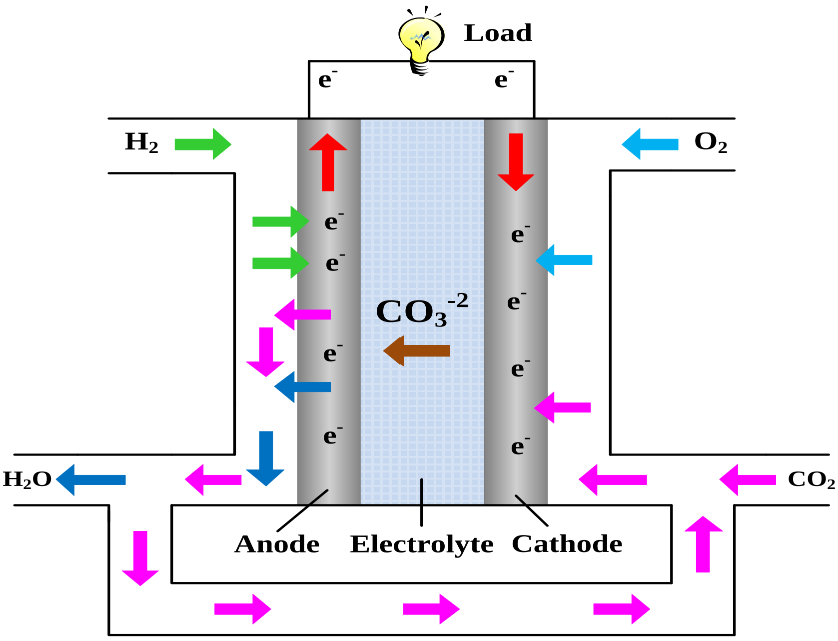

Figure 1. Schematic diagram of how MCFC works

2.2 Two Stage Cogeneration System of Molten Carbonate Fuel Cell

Part of the waste heat generated by MCFC is released directly to the environment through heat transfer, and this part of heat can be given by the following equation

$$Q_{loss} = \alpha A_l \left(T - T_0\right), \quad (5)$$

Where α denotes convective heat transfer coefficient, A_l represents the effective heat transfer area. Combined with the previous analysis, it can be obtained that the waste heat flow rate generated by MCFC can be reused is

$$
\begin{aligned}
\dot{q}_h &= -\Delta \dot{H} - \dot{P}_{cell} - \dot{Q}_{loss} - \dot{Q}_{re} \\
&= -\frac{\Delta h}{n_e F} jA - U_{cell} jA - \alpha A_l \left(T - T_0\right) - k_{re}\left(1-\varepsilon\right)\left(T - T_0\right)
\end{aligned}
\tag{6}
$$

Stirling cycle as one of the important standard air circulation heat engine, its main advantage is that the cycle can be driven by a variety of fuels, whether liquid, gaseous or solid, it can use almost any fuel as a high temperature heat source Therefore, Stirling heat engine as a fuel cell secondary power generation device is one of the most suitable choice for MCFC. A complete Stirling cycle consists of four reversible processes: isothermal heat transfer, isothermal heat transfer, isothermal heat transfer and isothermal heat transfer:

(1) The constant temperature expansion process in which the high pressure and high temperature working medium pushes the piston to do external work while absorbing heat from the external heat source;

(2) Under the condition of constant volume, the high-temperature working medium carries out the process of constant volume heat release to the regenerator, and the pressure and temperature are reduced correspondingly and return to the initial state, thus completing a closed cycle;

(3) The process in which the low-pressure and low-temperature working medium receives constant temperature compression of the piston while releasing heat from the external cold source;

(4) When the low-temperature working medium is heated by the regenerator at constant volume, the pressure and temperature rise correspondingly.

The two isothermal processes are heat absorption from the high temperature heat source and heat release to the low temperature heat source, while the heat of the two isobaric processes is heat recovery inside the cycle, that is, the isobaric process absorbs the heat released by the isobaric process. So this cycle is a reversible cycle between a hot reservoir and a cold reservoir.

For a given input heat flow $\dot{q}_h$, considering the finite heat conductivity and the actual irreversibility of the heat recovery in the engine, then the maximum efficiency of the Stirling engine can be expressed as [24]

$$
\eta_{engine} = \frac{\dot{q}_n / K + (a-1)T - aT_0 + T_e}{2aT + a\left[q_n / K + (a-1)T - aT_0 + T_e\right]} , \tag{7}
$$

Where $a = xC / \left[R\ln\left(V_2/V_1\right)\right]$ refers to the irreversible finite heat conductivity of a heat engine, $T_e = \left\{\left[(a+1)T + aT_0 - q_h/K\right]^2 - 4a(a+1)TT_0\right\}^{0.5}$, $K = k_1 \Big/ \left[(1+b)\left(1+\sqrt{k_1/k_2}\right)^2\right]$, x is the ideal heat recovery fractional deviation, b is the time ratio of the regenerative part of the isothermal branch, C is the heat capacity per mole of working material involved in the regenerative process, k_1 and k_2 are the thermal conductivity between the working material and the heat source at temperature T (operating temperature of MCFC) and temperature T_0 (ambient temperature) respectively. *Kt* is the thermal conductivity between the working material and the heat source at temperature (operating temperature of MCFC) and temperature (ambient temperature) respectively

$$\eta_{engine} = \frac{a_1\left(1-\eta_{cell}\right)j-\left(T-T_0\right)\left(a_2+a_3\right)+\left(a-1\right)T-aT_0+T_e}{2aT+a\left[a_1\left(1-\eta_{cell}\right)j-\left(T-T_0\right)\left(a_2-a_3\right)+\left(a-1\right)T-aT_0+T_e\right]}, \quad (8)$$

and

$$P_{engine} = -\frac{A\Delta h}{a_1 n_e F}\left[a_1\left(1-\eta_{cell}\right)j-\left(T-T_0\right)\left(a_2+a_3\right)\right]$$
$$\times\frac{a_1\left(1-\eta_{cell}\right)j-\left(T-T_0\right)\left(a_2+a_3\right)+\left(a-1\right)T-aT_0+T_e}{2aT+a\left[a_1\left(1-\eta_{cell}\right)j-\left(T-T_0\right)\left(a_2+a_3\right)+\left(a-1\right)T-aT_0+T_e\right]}, \quad (9)$$

Where $a_1 = -\frac{A\Delta h}{n_e FK}$ refers to the comprehensive parameters of the system structure, and $a_2 = \frac{\alpha A_l}{K}$ and $a_3 = \frac{k_{re}}{K}\left(1-\varepsilon\right)$ are two parameters used to characterize the influences of the heat-leak irreversibility from the fuel cell to the surroundings and non-perfect regeneration in the regenerator on the performance of the hybrid system.

Thus, the efficiency and output power of the whole coupling system can be obtained, namely,

$$\eta_{hybrid} = \frac{P_{hybrid}}{\dot{Q}_{all}} = \frac{P_{cell}+P_{engine}}{-\Delta\dot{H}}$$
$$= \eta_{cell}+\eta_{engine}\times\left[1-\eta_{cell}-\left(T-T_0\right)\left(\frac{a_2}{a_1 j}+\frac{a_3}{a_1 j}\right)\right], \quad (10)$$

and

$$P_{hybrid} = \eta_{hybrid}\left(-\Delta\dot{H}\right)$$
$$= -\frac{jA\Delta h}{n_e F}\left\{\eta_{cell}+\eta_{engine}\times\left[1-\eta_{cell}-\left(T-T_0\right)\left(\frac{a_2}{a_1 j}+\frac{a_3}{a_1 j}\right)\right]\right\}。 \quad (11)$$

It can be seen from equations (10) and (11) that the efficiency and output power of the coupled system are respectively composed of two parts. The first part is the output energy efficiency of the fuel cell itself, while the second part, obviously, represents the output energy efficiency after Stirling engine is involved. Figures 2 and 3 clearly show that after coupling the secondary energy device, the overall performance of the coupled system is superior to that of the single fuel cell output, and both efficiency and power have been significantly improved. At the same time, the performance of the system is also directly related to the operating temperature, what is clear is that: when the fuel cell operating temperature increases, the system performance is better, but increasing the operating temperature is not a way that can be used indefinitely, because the machine itself is limited to the temperature tolerance, in order to ensure the safe and stable operation of the fuel cell system, the allowable range of temperature cannot be increased indefinitely. The fuel cell must operate at a suitable and safe temperature range. Obviously, coupling a secondary energy efficiency device is an important means to improve energy efficiency performance. Similar methods, coupling different secondary engines, such as Braysson engine [25] and Carnot engine [26], can also be used to achieve the same purpose. However, the Stirling engine studied in this paper is considered as a unique engine because its theoretical efficiency is almost equal to the theoretical maximum efficiency. Next, we will discuss each energy efficiency parameter in more depth to provide a more complete energy efficiency management plan.

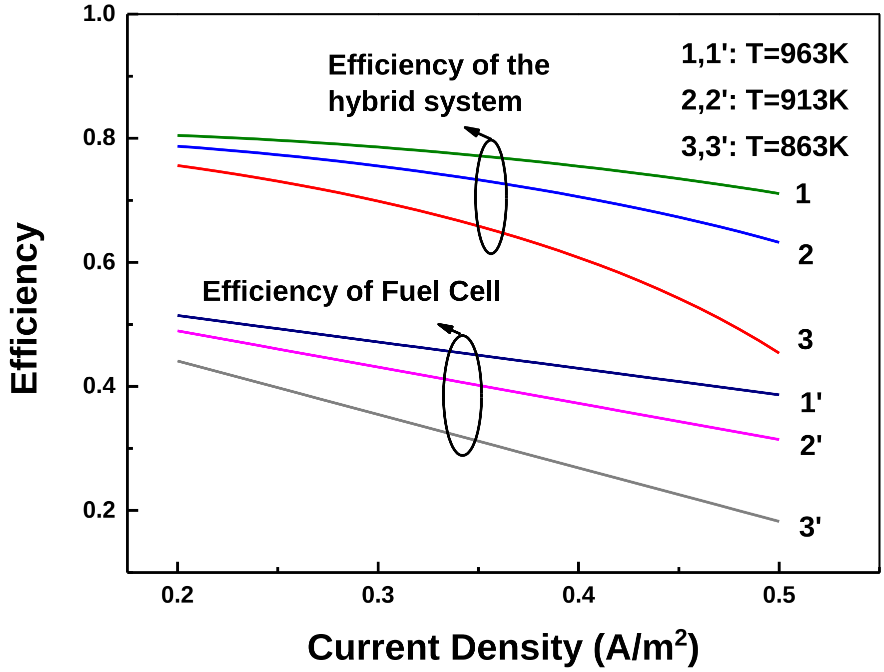

Figure 2. The curve of efficiency with current density at different operating temperatures.

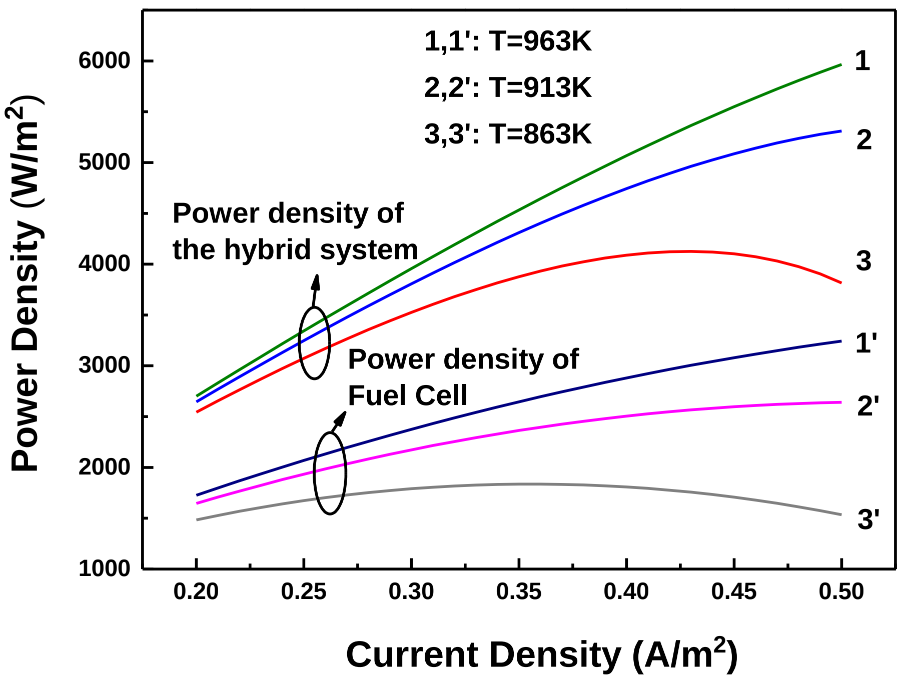

Figure 3. The curve of power density with current density at different operating temperatures.

3. ANALYSIS OF ENERGY EFFICIENCY MANAGEMENT

Figures 4 and 5 show the three-dimensional curves of efficiency and output power as the current density and temperature change accordingly. It can be easily observed from the figure that the performance of the whole coupled system will increase first and then decrease with the increase of current density, that is to say, the efficiency and output power of the system have an extreme point respectively, and the system performance is optimal at the corresponding point. In addition, it can be seen more clearly from figure 6 that the current density corresponding to the maximum efficiency and maximum power is not the same for the same system. Then which current density should be used as the working current in practice? This depends on whether the user prefers efficiency or power, which will be discussed in more detail later on.

From Figures 4 and 5, it can also be noted that the performance of the system will be improved with the increase of the fuel cell operating temperature. Meanwhile, the maximum efficiency, maximum power density and corresponding current density will be slightly increased with the increase of the fuel cell operating temperature. In general, the reactant temperature at the inlet of a coupling system is usually higher than the ambient temperature, because the reactants supplied to the system tend to be highly compressed normally, and it is assumed that the reactant temperature is equal to the ambient temperature when the reactants supplied are at one atmosphere pressure. The inlet temperature of the reactants may reduce the operating temperature of the MCFC, and the lower operating temperature will also drag down the performance of the overall coupling system, so it is easy to predict that the performance of the coupling system will improve with the increase of operating temperature. Moreover, as to how to choose the operating temperature of the system, the thermal stability required in the process of manufacturing MCFC, the investment cost and material degradation of the whole system that can operate at the specified temperature should be taken into account. This is a very complex subject that needs to be studied separately and is not the focus of this paper. At present, the reasonable operating temperature range of molten carbonate fuel cell is about 800~1200K [2].

Figure 7 reflects the relation curve between power and efficiency, which can be used to better discuss the difference between efficiency preference and power preference. In the figure, there exists a maximum efficiency $\eta_{\max}$ and a maximum power density $P^*_{\max}$, P^*_m and η_{m} represent the corresponding power density at the highest efficiency and the corresponding efficiency at the highest output power respectively. These four values correspond to the upper and lower boundaries of power and efficiency that can be selected. When the efficiency is at its maximum value $\eta_{\max}$, the corresponding power value P^*_m gives the lower limit of power selection. When the power is maximized, the corresponding efficiency value η_{m} gives the lower limit of efficiency selection. Therefore, it can be concluded that the selected performance range is:

$$P^*_m < P^* < P^*_{\max} \tag{12}$$

$$\eta_{\mathrm{m}} < \eta < \eta_{\max} \tag{13}$$

The current density ranges that can be selected are:

$$j_\eta \le j \le j_{P^*} \tag{14}$$

For users with efficiency preference, they have to accept the loss of part of power as the cost, and the working current of the fuel cell is j_η. Similarly, for users with power preference, they have to accept the loss of part of efficiency as the cost, and the working current of the fuel cell is j_{P^*}. Therefore, in engineering, the power preference or efficiency preference of engineers determines the choice of working current. Of course, users with moderate preferences can choose any of the values in equations (12)-(14). It has to be said that the three values are actually mutually dependent. When one of the values is determined, the other two are determined accordingly. In addition, it can be seen from Figure 7 that the performance of the system is closely related to the ambient temperature. Through the proportional relationship, it can be found that the ambient temperature has an impact on the overall performance, but compared with the waste heat utilization, this impact is insignificant.

Similar results can also be found for other types of fuel cell coupling systems, such as direct carbon fuel cell (DCFC) [27] and solid oxide fuel cell (SOFC) [28] coupling system. Table 2 lists the performance of three different types of fuel cell coupled Stirling thermal engine systems at the same operating temperature. The comparison shows that the performance of solid oxide fuel cell is the best under the same working temperature, and solid oxide fuel cell is indeed the favorite of various kinds of fuel cell research. However, the advantages of MCFC lie in the high operating temperature, fast reaction speed, relatively low requirements on the purity of fuel, fuel can be reformed in the cell, no precious metal catalyst, low cost, liquid electrolyte, easy to operate. At the same time, the performance of MCFC studied in this paper is relatively better than that of DCFC.

Table 2. Four key performance points of three typical fuel cells-Stirling engines coupling system at the same operating temperature.

	$\eta_{\max}$	$P^*_{\max}$	η_{m}	P^*_m
MCFC	78%	5869W/A	60%	1598W/A
DCFC	83%	496W/A	62%	79W/A
SOFC	86%	14953W/A	59%	1436W/A

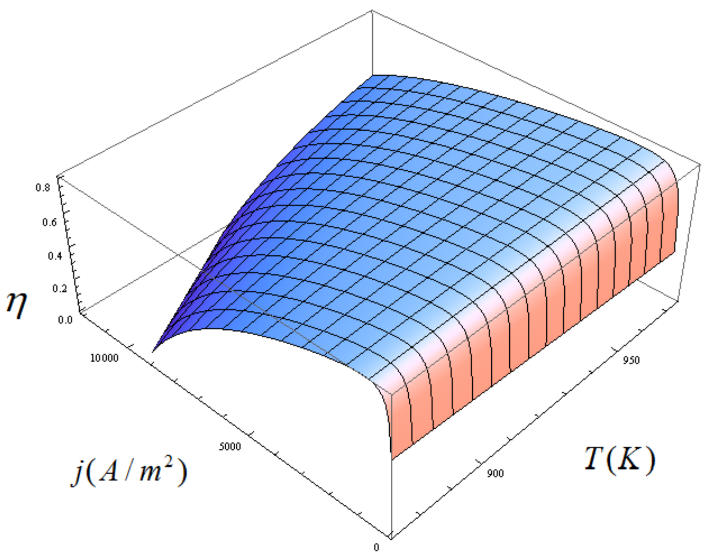

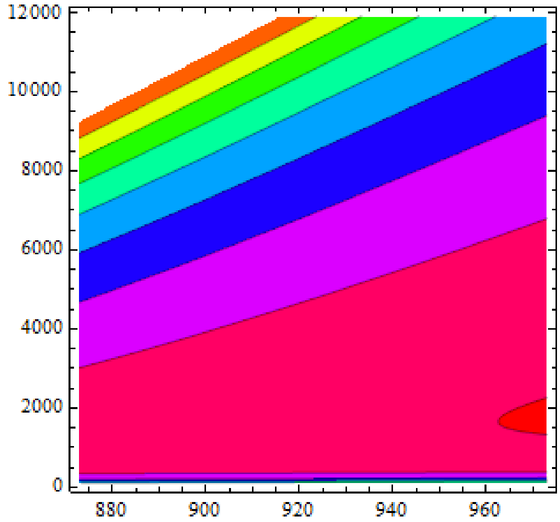

Figure 4. Three-dimensional diagram of efficiency as temperature and current density change.

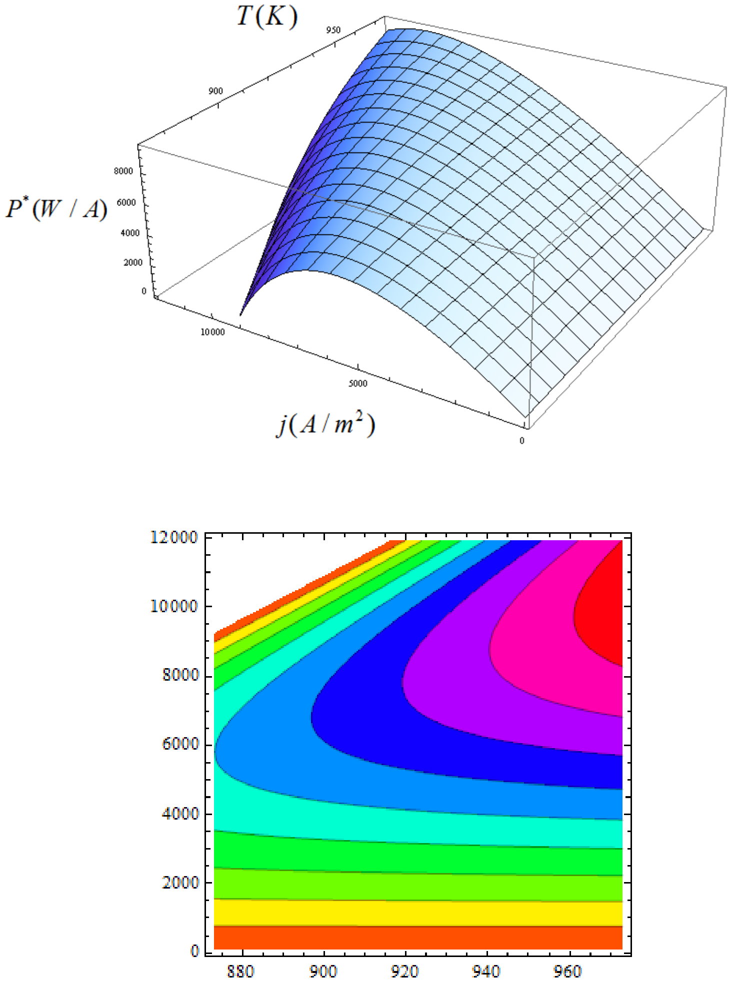

Figure 5. Three-dimensional diagram of power density as temperature and current density change.

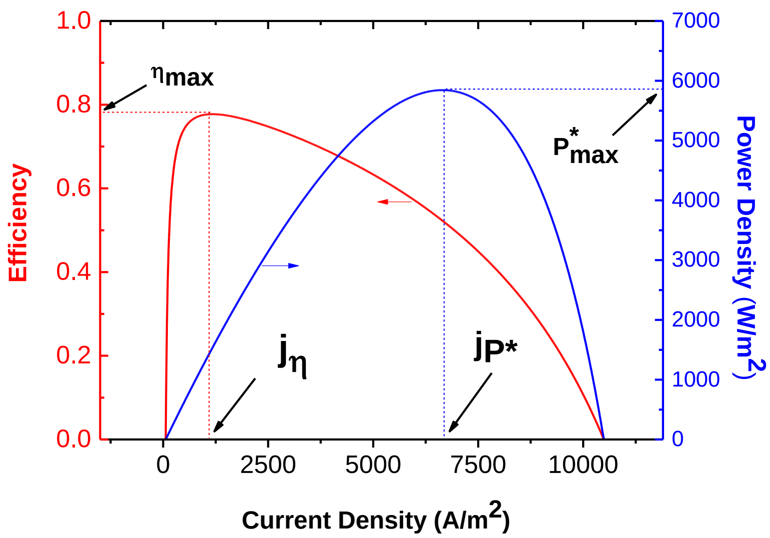

Figure 6. The efficiency and power of a coupled system as a function of current density.

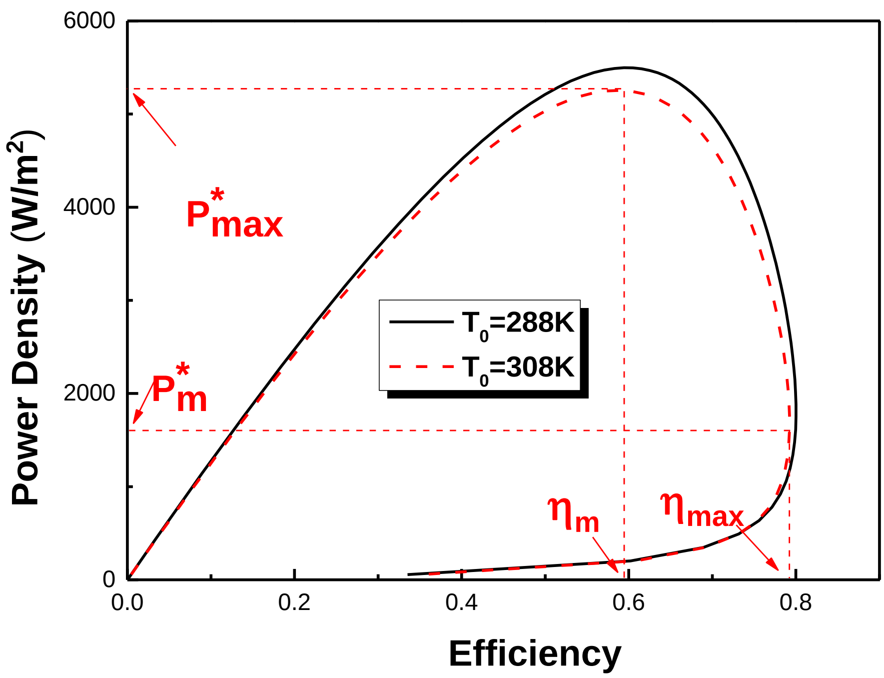

Figure 7. The relationship between efficiency and power of a coupling system.

4. CONCLUSION

The focus of this paper is to achieve the best energy efficiency management of MCFC working process, through the coupling of bipolar energy device (Stirling engine) method, greatly improve the performance of molten carbonate fuel cell system. By means of electrochemistry and non-equilibrium thermodynamics, the analytical expressions of efficiency and power output of the fused carbonate fuel cell coupled thermo-mechanical power system are obtained. In addition, the upper and lower limits of efficiency and output power are determined by strict numerical calculation. The reasonable performance range of the coupling system of molten carbonate fuel cell is analyzed, and the optimal energy efficiency management scheme is given. The results obtained may provide some theoretical basis for the optimal design and practical operation of MCFC coupling system. At the same time, this method can be easily extended to other kinds of fuel cell coupling system.

ACKNOWLEDGEMENTS
This work was supported by the National Nature Science Foundation of China (No.11804189).

References

1. Y. Wang, B. Seo, B Wang, N. Zamel, K. Jiao and X.C. Adroher, *Energy and AI*, 1 (2020) 100014.
2. J. Wang, H. Wang and Y. Fan, *Engineering*, 4 (2018) 352.
3. M. Muthukumar, N. Rengarajan and B. Velliyangiri, *Mater. Today: Proc.*, 45 (2021) 1181.
4. P. Ahmadi, S.H. Torabi, H. Afsaneh and Y. Sadegheih, *Int. J. Hydrogen Energy*, 45 (2020) 3595.
5. T.B. Ferriday and P.H. Middleton, *Int. J. Hydrogen Energy*, 46 (2021) 18489.
6. P. Ren, P. Pei, Y. Li, Z. Wu, D. Chen and S. Huang, *Prog. Energy Combust. Sci.*, 80 (2020) 100859.
7. A. Baroutaji, T. Wilberforce and M. Ramadan, *Renewable Sustainable Energy Rev.*, 106 (2019) 31.
8. E. Ogungbemi, O. Ijaodola, F.N. Khatib and T. Wilberforce, *Energy*, 172 (2019) 155.
9. Y. Hames, K. Kaya, E. Baltacioglu and A. Turksoy, *Int. J. Hydrogen Energy*, 43 (2018) 10810.
10. S. Chen, M. Li, M. Gao, J. Jin and M.A. van Spronsen, *Nano letters*, 20 (2020) 1974.
11. I. Gajda, J. Greenman, I.A. Ieropoulos, *Curr. Opin. Electrochem.*, 11 (2018) 78.
12. X. Lü, Y. Wu, J. Lian, Y. Zhang, C. Chen and P. Wang, *Energy Convers. Manage.*, 205 (2020) 112474.
13. Y. Zhao, B.P. Setzler, J. Wang, J. Nash, T. Wang and B. Xu, *Joule*, 3 (2019) 2472.
14. I.S. Sorlei, N. Bizon, P. Thounthong and M. Varlam, *Energies*, 14 (2021) 252.
15. G. Wang, Y. Yu, H. Liu, C. Gong, S. Wen and X. Wang, *Fuel Process. Technol.*, 179 (2018) 203.
16. S. Ahmadi, S.M.T. Bathaee and A.H. Hosseinpour, *Energy Convers. Manage.*, 160 (2018) 74.
17. Z. Fu, L. Zhu, F. Tao, P. Si and L. Sun, *Int. J. Hydrogen Energy*, 45 (2020) 8875.
18. Y. Wang, Z. Sun and Z. Chen, *Applied energy*, 254 (2019) 113707.
19. H. Li, A. Ravey, A. N'Diaye and A. Djerdir, *Energy Convers. Manage.*, 192 (2019) 133.
20. Y. Liu, J. Li, Z. Chen, D. Qin and Y. Zhang, *J. Power Sources*, 429 (2019) 55.
21. H. Zhang, G. Lin and J. Chen, *Int. J. Hydrogen Energy*, 36 (2011) 4015.
22. Y. Shin, W. Park, J. Chang and J. Park, *Int. J. Hydrogen Energy*, 32 (2007) 1486.
23. E. Akrami, M. Ameri and M. V. Rocco, *Energy*, 227 (2021), 120511.
24. J. Chen, Z. Yan and L. Chen, *Int. J. Energy Res.*, 22 (1998) 805.
25. L. Chen and Y. Lin, *Int. J. Electrochem. Sci.*, 15 (2020) 149.
26. L. Chen, S. Gao and H. Zhang, *Int. J. Electrochem. Sci.*, 9 (2014) 5788.
27. L. Chen, L. Gao and Y. Lin, *Int. J. Electrochem. Sci.*, 15 (2020) 4908.
28. L. Chen, H. Zhang, S. Gao and H. Yan, *Energy*, 64 (2014) 923.